Heterogeneous Catalysis Hot Paper

DOI: 10.1002/anie.201306899

Size-Dependent Phase Transformation of Catalytically Active Nanoparticles Captured In Situ**

*Nico Fischer, Brett Clapham, Theresa Feltes, Eric van Steen, and Michael Claeys**

Abstract: *The utilization of metal nanoparticles traverses across disciplines and we continue to explore the intrinsic size-dependent properties that make them so unique. Ideal nanoparticle formulation to improve a process's efficiency is classically presented as exposing a greater surface area to volume ratio through decreasing the nanoparticle size. Although, the physiochemical characteristics of the nanoparticles, such as phase, structure, or behavior, may be influenced by the nature of the environment in which the nanoparticles are subjected[1,2] and, in some cases, could potentially lead to unwanted side effects. The degree of this influence on the particle properties can be size-dependent, which is seldom highlighted in research. Herein we reveal such an effect in an industrially valuable cobalt Fischer–Tropsch synthesis (FTS) catalyst using novel in situ characterization. We expose a direct correlation that exists between the cobalt nanoparticle's size and a phase transformation, which ultimately leads to catalyst deactivation.*

Fischer–Tropsch synthesis (FTS) is a surface polymerization reaction producing a range of valuable hydrocarbon products from synthesis gas (syngas; a mix of H_2 and CO) and with the industrial output of FTS increasing, so is the necessary research to improve the process.[3,4] In case of supported cobalt nanoparticles, a major focus of current research is relating ideal activation to a distinct nanoparticle size.[5–7] Owing to the presence of both oxidizing and reducing compounds during FTS, similar to many other commercial reactions utilizing nanocrystallite catalysts,[8] an important alternative in studying nanoparticle size effects is exploring certain forms of deactivation that can also be crystallite size-dependent. For FTS, it is argued that kinetically water, the potentially oxidizing species, does not play a role,[9,10] however, numerous reports hypothesize it does promote deactivation. This includes a rather broad range of mechanisms including re-oxidation to CoO, the promotion of cobalt-support interactions such as the formation of cobalt aluminates, H_2O aided sintering, or surface reconstruction.[11–14] It is through re-oxidation that we can begin to focus on crystallite size-dependence. Yet, this conditional phase transformation has only been studied theoretically[12] or only been proposed using indirect methods which do not monitor the oxidation of the cobalt directly, that is, with ex situ characterization techniques[14] with no solid conclusion to date.

Cobalt's sensitivity to re-oxidation by air is the leading obstacle to this research. To overcome this, we introduce two complementary in situ techniques developed in our laboratory to study the catalyst nanoparticles. An advantage in studying ferromagnetic materials is that it is possible to distinguish the intrinsic properties, which occur in the nanoparticles as their crystallite size and phase changes. Herein, we report a novel in situ magnetometer that is capable of monitoring the magnetic cobalt catalyst at high temperatures and pressures during activation (e.g. the reduction of Co_3O_4 to the active metallic Co^0 phase) and reaction, thus, giving insight into the catalysts' composition and crystallite size.[15] X-ray diffraction (XRD) is a common tool for materials science, but by supplying a new capillary cell reactor[16] we can monitor the crucial phase and crystallite size changes, which can occur rapidly, in operando and importantly in the presence of high water concentrations. Model-like cobalt catalysts supported on an industrially relevant alumina support material were studied with these techniques. The Co_3O_4 nanoparticles were synthesized by the reverse micelle technique, which yields crystallites with a narrow size distribution as we previously reported.[17] The sample names reflect their reduced metallic cobalt crystallite sizes from XRD measurements (additional characterization results can be found in the Supporting Information, Table S1).

Our initial experiments focused on in situ magnetic measurements (Figure 1a) of the two catalysts, CAT 9.5 (5.0 wt.% Co) and CAT 4.5 (1.8 wt.% Co). Full details on the background and experimental details of the technique can be found in the Supporting Information. Briefly, owing to the magnetic properties of the cobalt species, at temperatures higher than 13 °C, the only magnetic cobalt species present is metallic cobalt, Co^0 (see Table S2). This situation allowed us to measure and monitor the degree of reduction (DOR) throughout high-temperature activation in H_2 and during the reaction (conditions listed in Table S3). This monitoring was mainly done by taking magnetic measurements at an external field strength of 20 kOe then at 0 kOe to assess the amount of metallic cobalt and the remnant magnetization, respectively. Only metallic crystallites with a size larger than a critical diameter (depending on conditions and crystallite phase 7–20 nm)[4,18] will retain a level of magnetization after removal

[*] Dr. N. Fischer, B. Clapham, Dr. T. Feltes, Prof. Dr. E. van Steen, Prof. Dr. M. Claeys
Centre for Catalysis Research and c*change (DST-NRF Centre of Excellence in Catalysis), Department of Chemical Engineering
University of Cape Town
Cape Town (South Africa)
E-mail: michael.claeys@uct.ac.za

[**] This work is supported by the Centre for Catalysis Research at the University of Cape Town and c*change (DST-NRF Centre of Excellence in Catalysis). We also thank J. Macke, M. Wüst, and C. de Vries for their contributions to the work and Sasol R&D for support of the development of the in situ magnetometer.

Supporting information for this article is available on the WWW under http://dx.doi.org/10.1002/anie.201306899.

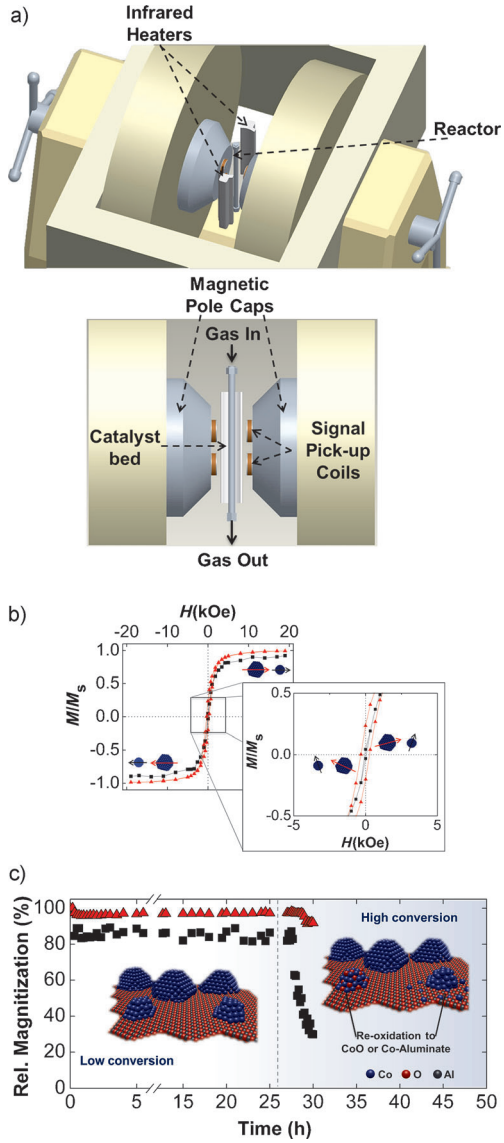

Figure 1. a) Diagram of the in situ magnetometer with a maximum operating external field strength of 20 kOe and capable of operation at 50 bar and 600 °C. b) The full hysteresis of CAT 9.5 red, CAT 4.5 black after reduction of the cobalt nanoparticles in H_2, and an expansion of the plot around no external field ($H = 0$ kOe). c) The relative magnetization (normalized with respect to initial magnetization) at maximum field as a function of time on stream during low-conversion FTS ("no" water/$X_{CO} < 10\%$) at 190 °C and 10 bar syngas for the first 25 h (Inset: picture showing stable cobalt crystallites on the alumina support) and subsequent with 3 h of FTS with an additional 6 bar H_2O co-feeding, simulating 67% CO conversion red ▲ CAT 9.5, black ■ CAT 4.5 (Inset: picture showing the re-oxidation of small cobalt crystallites to CoO or cobalt aluminates).

of the external magnetic field. Smaller crystallites of metallic cobalt will display superparamagnetic behavior. This means that these crystallites are so small they behave like dipoles (paramagnetism) and show no remnant magnetization once the external magnetic field is removed.[19] In addition, between reduction and reaction stages, we measured a full hysteresis from −20 kOe to 20 kOe in an argon atmosphere at 190 °C (Figure 1 b). This gave us a real insight to the sizes of our nanoparticles. Magnetization at lower external field strengths (H) is dominated by larger metallic cobalt crystallites and this is exquisitely demonstrated by the hysteresis behavior in CAT 9.5 as opposed to the superparamagnetic behavior of CAT 4.5 (see expansion in Figure 1 b).

By using the Langevin function [Eq. (S1)],[19] which is only valid for superparamagnetic samples and, thus, can only be applied for CAT 4.5, we were able to rationalize the volume weighted crystallite size distribution for CAT 4.5 (Figure S2 a). This approach gave an average Co^0 crystallite size of 5.1 nm after reduction, which correlated well with the TEM and XRD measurements of the reduced cobalt catalyst as previously reported.[17] In addition, and in contrast to CAT 9.5, the incomplete saturation ($M/Ms \leq 1$) in CAT 4.5 further supports that it consists of smaller Co^0 crystallites, since the measurement of magnetization is strongly dependent on crystallite size and smaller crystallites require a higher external field strength to be magnetized.[19]

With the magnetic measurements indicating that each catalyst contains Co^0 crystallites of differing average size, we exposed both samples to syngas ($CO + H_2$) at 10 bar and 190 °C for 25 h of low-conversion (less than 10%) FTS conditions, later referred to as the "base case" (Table S3). After this, keeping the syngas at 10 bar, we supplied an additional 6 bar of water partial pressure by the addition (co-feeding) of water vapor to the reactor inlet gas stream (total pressure 16 bar), simulating 67% industrially relevant CO conversions (Figure S1). Note that with this experimental approach and the high space velocity applied, the syngas conversion levels are very low (10% and smaller) and the associated water partial pressure is negligible. Consequently, the partial pressure of syngas is constant along the length of the catalyst bed. The addition of water at correspondingly increased total pressure simulates high conversion conditions, again with constant partial pressures of syngas without diluting the synthesis gas. It was previously shown that replacing co-fed water with argon resulted in catalyst performance (activity and selectivity) at base case conditions without co-feeding.[20] Therefore an increase in reactor pressure through additional P_{H_2O} will give direct and unperturbed information on the influence of water on the catalytic behavior. We continuously measured the magnetization throughout the experiment. For both model catalysts, the magnetization relative to the initial magnetization at maximum field (Figure 1 c) decreased very slightly in the first 5–10 min on stream. This change is possibly a result of a re-oxidation and/or a carbidization effect during surface reconstruction[14,21] of the metallic cobalt crystallites upon first exposure to synthesis gas. However, after this initial decrease, the magnetization remains stable during the first 25 h of the experiment. This result complements the weight percentage of the metallic cobalt present as crystallites larger than the critical diameter (in contrast to superparamagnetic behaving crystallites), which also does not change upon the first 25 h of exposure to FTS conditions (Figure S3).

Proceeding to simulate high-conversion conditions through the exposure of an additional 6 bar water partial pressure, both catalysts' relative magnetization decreased, but while the magnetization of CAT 9.5 only dropped slightly,

CAT 4.5 declined continuously. This result is a strong indication of metallic cobalt, Co^0, re-oxidizing to the Co^{2+} state in the presence of water and implies re-oxidation is indeed more feasible for smaller crystallites. With additional hysteresis measurements, crystallite size distributions for CAT 4.5 showed unchanged average sizes of 5.1 nm in the reduced state and 5.0 nm after 25 h under low-conversion FTS conditions (calculated distributions are in Figure S2). Under simulated high-conversion conditions, the increase of the percentage of large crystallites was obtained with this catalyst is most likely due to a "loss" of small metallic crystallites through oxidation or sintering (note that a crystallite size distribution cannot be determined for non-superparamagnetic samples using the Langevin approach). However, in this study, re-oxidation to either CoO or a cobalt–aluminate species seems to be the dominating effect. Furthermore, the average crystallite size of the spent metallic Co particles in CAT 9.5 as determined by ex situ XRD was 10.5 nm, exhibiting negligible growth. Therefore, the increase in ferromagnetic material is believed to be the result of smaller Co^0 crystallites being re-oxidized while the larger crystallites remain in their metallic state.

To validate this investigation, we performed a re-oxidation threshold-type experiment with an in situ XRD capillary cell (Figure 2a), with which we could directly monitor the rapid changes in the cobalt phases. Importantly, the cell design with its heated feed and product lines allowed co-feeding of high levels of water so that the same experimental approach as described above could be applied. Prior to FTS experiments, the catalysts, CAT 18.9 (6.4 wt.% Co) and CAT 4.1 (4.0 wt.% Co) (Co weight loadings were slightly higher to produce resolvable XRD patterns), were reduced in situ in H_2 (Table S3) and we recorded the transformations by continuous XRD scans. It was observed that CAT 4.1 was more facile to reduce (DOR = 95%) and underwent phase changes from $Co_3O_4 \rightarrow CoO \rightarrow Co^0$ at slightly lower temperatures than CAT 18.9 (Figure S5) and although CAT 18.9 still presented observable amounts of CoO (DOR = 91%), for the purpose of the experiment the importance lies in that the two catalysts consisted of distinct cobalt crystallite sizes (4.1 and 18.9 nm) and contained a purely fcc metallic cobalt phase.

Immediately after reduction, we again subjected the catalysts to low-conversion (less than 10%) FTS conditions at 220°C at atmospheric pressure (Table S3). To monitor when/if re-oxidation occurred we kept the syngas partial pressure constant at 1 bar and incrementally increased the water partial pressure, P_{H_2O}, to 0.5, 1, 2, and 3 bar while raising the total pressure correspondingly (i.e. 1.5, 2, 3, and 4 bar). Each stage was held for 3 h and continuously monitored. The calculated ratios of the partial pressures, $P_{H_2}P_{H_2O}$, correlate to simulated CO conversions of 62.5, 76.9, 87, and 91%, respectively (Figure S1). The resulting in situ XRD scans from CAT 18.9 (Figure 2b) showed neither phase changes from fcc-Co^0, even when looking closer at the refined crystallite sizes of each spectrum (Figure S4a), nor significant crystallite growth. This led to the principal result from the experiment with CAT 4.1 (Figure 2c). The rapid oxidation of metallic cobalt is difficult to capture and near impossible with ex situ techniques. Herein we observed that a phase change indeed occurred at higher P_{H_2O}, that is, higher simulated CO conversions. Initially, the metallic fcc-Co^0 phase is stable, even upon the addition of 0.5 bar H_2O (or 62.5% conversion), although some re-oxidation is evident. It is the measurement at 1 bar H_2O (or 76.9% conversion) where we observed what appeared to be complete re-oxidation to CoO. From this point forward, CoO remained the stable phase at even higher P_{H_2O}. Again, from the crystallite size refinements (Figure S4b), after exposure to 0.5 bar H_2O we recorded an average Co^0 crystallite size of 3.5 nm. Upon which, after exposure to the 76.9% simulated conversion conditions, there was a slight growth in the crystallites as they converted into CoO.

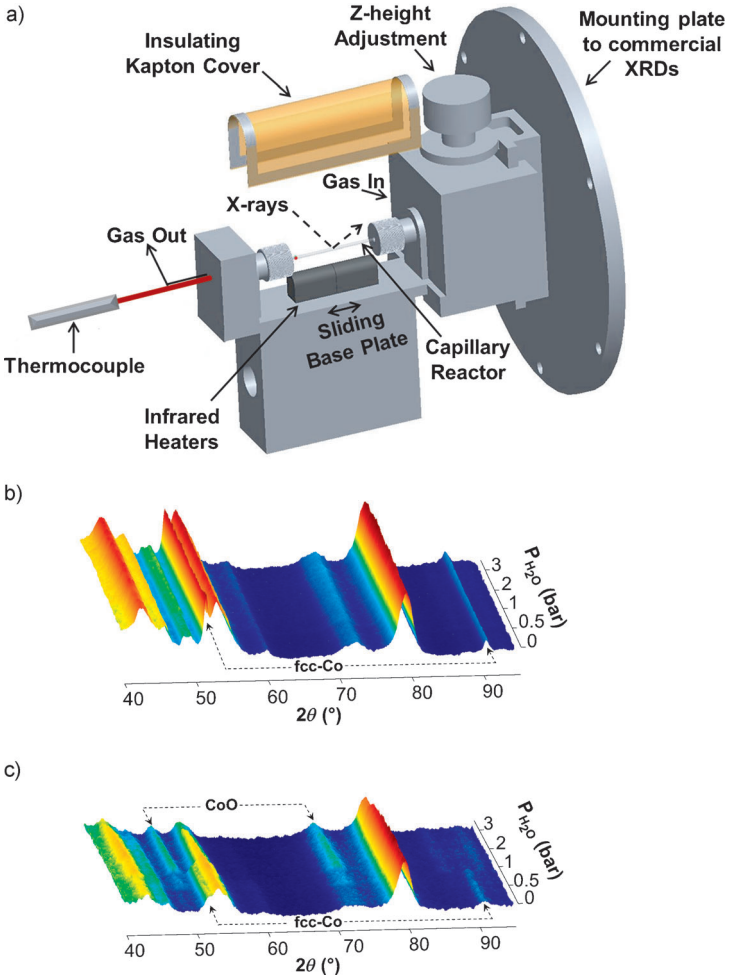

Figure 2. a) Design of the in situ capillary cell reactor. The catalyst bed is placed inside a capillary cell centered between the infrared heaters and XRD beam path. An internally placed thermocouple measures and controls the temperature of the catalyst bed through infrared heating. In situ XRD patterns for b) CAT 18.9, and c) CAT 4.1, recorded during FTS at 220°C and 1 bar syngas while increasing P_{H_2O} from 0 to 3 bar to simulate high-conversion reaction conditions.

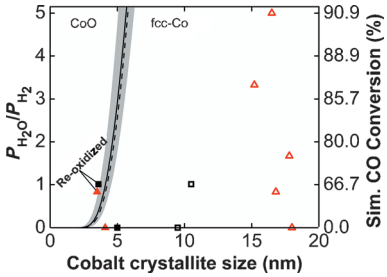

Figure 3. Metallic cobalt crystallite sizes (prior to re-oxidation in the case of the small crystallites) from FTS experiments at corresponding simulated high CO conversions. Magnetic characterization: ■ CAT 4.5, □ CAT 9.5; XRD characterization: red ▲ CAT 4.1, red △ CAT 18.9. (All symbols belong to both *y*-axes. The PH_2O/PH_2 ratio and the simulated CO conversion are directly dependent values). Data is superimposed on the thermodynamic stability region for fcc-Co: —— 220 °C, ----- 190 °C, and the shaded area represents a 10% surface-energy margin (adapted from van Steen et al.).[12]

Correlating the in situ magnetic and XRD results to the theoretical work on the crystallite size dependence in the re-oxidation of cobalt crystallites done by van Steen et al.,[12] we present the most supportive experimental evidence that confirms this phase transformation is strongly size dependent (Figure 3). The significance in this result is that in pursuing the development of an ideal cobalt FTS catalyst, the industrial CO conversion lies readily above 60% and in that realm a percentage of metallic cobalt could possibly be lost to re-oxidation. It is likely this is not the most influential route to deactivation of an industrial cobalt FTS catalyst, but could be so in other reactions with similar environments utilizing metal nanoparticles.

Using the example of Fischer–Tropsch catalysis, this work demonstrates that metal nanoparticles can exhibit phase transitions that are dependent on their crystallite size. Such processes are, likely to occur in various other applications, and not only catalytic ones. Thus, with the overall investigation into the intrinsic properties of novel metal nanoparticles, applying additional efforts into understanding crystallite size-dependent phase transformations can give a fundamental understanding of nanomaterials and their ultimate function.

Experimental Section

Materials: The supported Co_3O_4 nanocrystallites were synthesized by the reverse micelle microemulsion technique as reported elsewhere[18] and detailed in the Supporting Information.

In-situ magnetic measurements were conducted using a low-frequency vibrating sample magnetometer with maximum field strength of 20 kOe. Throughout reduction and reaction conditions, measurements were taken at 20 and 0 kOe, while full hysteresis measurements from −20 to 20 kOe were taken at desired intervals.

In-situ XRD: analyses were performed using a capillary cell reactor (borosilicate o.d. 1 mm, wall thickness (w.t.) 0.02 mm, i.d. 0,96 mm) mounted on a Bruker D8 Advance diffractometer, equipped with a cobalt source ($\lambda_{K\alpha 1} = 0.178897$ nm) and a position sensitive detector. To maximize resolution and minimize the time required to perform each scan, all spectra were recorded between 40–95 2θ°. Full methods are available in the Supporting Information.

Received: August 6, 2013
Revised: September 23, 2013
Published online: December 13, 2013

Keywords: cobalt · Fischer–Tropsch · magnetic properties · phase transitions · size-dependent

[1] H. Zhang, B. Gilbert, F. Huang, J. F. Banfield, *Nature* **2003**, *424*, 1025 – 1029.
[2] D. V. Talapin, Y. Yin, *J. Mater. Chem.* **2011**, *21*, 11454 – 11456.
[3] E. de Smit, B. M. Weckhuysen, *Chem. Soc. Rev.* **2008**, *37*, 2758 – 2781.
[4] A. Y. Khodakov, W. Chu, P. Fongarland, *Chem. Rev.* **2007**, *107*, 1692 – 1744.
[5] G. L. Bezemer, J. H. Bitter, H. P. C. E. Kuipers, H. Oosterbeek, J. E. Holewijn, X. D. Xu, F. Kapteijn, A. J. van Dillen, K. P. de Jong, *J. Am. Chem. Soc.* **2006**, *128*, 3956 – 3964.
[6] G. Prieto, A. Martínez, P. Concepción, R. Moreno-Tost, *J. Catal.* **2009**, *266*, 129 – 144.
[7] A. Tuxen, S. Carenco, M. Chintapalli, C.-H. Chuang, C. Escudero, E. Pach, P. Jiang, F. Borondics, B. Beberwyck, A. P. Alivisatos, G. Thornton, W.-F. Pong, J. H. Guo, R. Perez, F. Besenbacher, M. Salmeron, *J. Am. Chem. Soc.* **2013**, *135*, 2273 – 2278.
[8] C. H. Bartholomew, R. J. Farrauto, *Fundamentals of industrial catalytic processes*, 2nd ed., Wiley, Hoboken, NJ, **2006**.
[9] I. C. Yates, C. N. Satterfield, *Energy Fuels* **1991**, *5*, 168 – 173.
[10] H. Schulz, M. Claeys, S. Harms, *Stud. Surf. Sci. Catal.* **1997**, *107*, 193 – 200.
[11] G. L. Bezemer, T. J. Remans, A. P. van Bavel, A. I. Dugulan, *J. Am. Chem. Soc.* **2010**, *132*, 8540 – 8541.
[12] E. van Steen, M. Claeys, M. E. Dry, J. van de Loosdrecht, E. L. Viljoen, J. L. Visagie, *J. Phys. Chem. B* **2005**, *109*, 3575 – 3577.
[13] G. Jacobs, P. M. Patterson, Y. Q. Zhang, T. Das, J. L. Li, B. H. Davis, *Appl. Catal. A* **2002**, *233*, 215 – 226.
[14] J. van de Loosdrecht, B. Balzhinimaev, J. A. Daimon, *Catal. Today* **2007**, *123*, 293 – 302.
[15] M. Claeys, E. van Steen, J. L. Visagie, J. van de Loosdrecht, PCT patent WO 2010/004419 A2, **2010**.
[16] M. Claeys, N. Fischer, PCT patent WO 2013/005180 A1, **2013**.
[17] N. Fischer, E. van Steen, M. Claeys, *Catal. Today* **2011**, *171*, 174 – 179.
[18] P. A. Chernavskii, J. A. Dalmon, N. S. Perov, A. Y. Khodakov, *Oil Gas Sci. Technol.* **2009**, *64*, 25 – 48.
[19] J. A. Dalmon in *Catalyst characterization: Physical techniques for solid materials* (Eds.: B. Imelik, J. C. Védrine), Plenum, New York and London, Chap. 21, **1994**.
[20] H. Schulz, E. vein Steen, M. Claeys, *Stud. Surf. Sci. Catal.*, *Vol. 81* (Eds.: H. E. Curry-Hyde, R. F. Howe), Elsevier, Amsterdam, **1994**, pp. 455 – 460.
[21] I. M. Ciobîcă, R. A. van Santen, P. J. van Berge, J. van de Loosdrecht, *Surf. Sci.* **2008**, *602*, 17 – 27.

